

Unsupervised Fish Trajectory Tracking and Segmentation

Alzayat Saleh*, Marcus Sheaves*, Dean Jerry*[†], and Mostafa Rahimi Azghadi*[†]

*College of Science and Engineering, James Cook University, Townsville, QLD, Australia

[†]ARC Research Hub for Supercharging Tropical Aquaculture through Genetic Solutions, James Cook University, Townsville, QLD, Australia

Abstract—Deep Neural Network (DNN) for fish tracking and segmentation based on high-quality labels is expensive. Alternative unsupervised approaches rely on spatial and temporal variations that naturally occur in video data to generate noisy pseudo-ground-truth labels. These pseudo-labels are used to train a multi-task deep neural network. In this paper, we propose a three-stage framework for robust fish tracking and segmentation, where the first stage is an optical flow model, which generates the pseudo labels using spatial and temporal consistency between frames. In the second stage, a self-supervised model refines the pseudo-labels incrementally. In the third stage, the refined labels are used to train a segmentation network. *No human annotations are used during the training or inference.* Extensive experiments are performed to validate our method on three public underwater video datasets and to demonstrate that it is highly effective for video annotation and segmentation. We also evaluate the robustness of our framework to different imaging conditions and discuss the limitations of our current implementation.

Index Terms—Vision Transformers, Computer Vision, Convolutional Neural Networks, Image and Video Processing, Underwater Videos, Machine Learning, Deep Learning.

I. INTRODUCTION

Automatic tracking and segmentation of individual fish have a wide variety of applications in ecological behavioural analysis [1–5]. Understanding and predicting animal motion in the wild would bring significant benefits in many research and industry domains [6–9]. However, the movement and motion of animals in their natural environments is highly complex. Multiple factors can contribute to the complexity of individual movements. The animals are not always visible in a video, which makes tracking and segmentation difficult. Multiple animals may be in the same video, complicating the segmentation task. These challenges often require advanced computational methods.

Several studies have tried to address these challenges [10–14]. Such studies rely heavily on pixel-level annotations to train or improve their Deep Neural Network (DNN). These annotations are expensive and time-consuming, especially for fish segmentation in the wild.

The key underlying assumption of most of the current automated methods [10, 15–17] is that the training data is usually paired with the ground truth that comes from a video that contains a large number of fish. Although ground truth is still expensive, obtaining a large number of video sequences is necessary, because achieving accurate results using a small number of sample videos is very difficult.

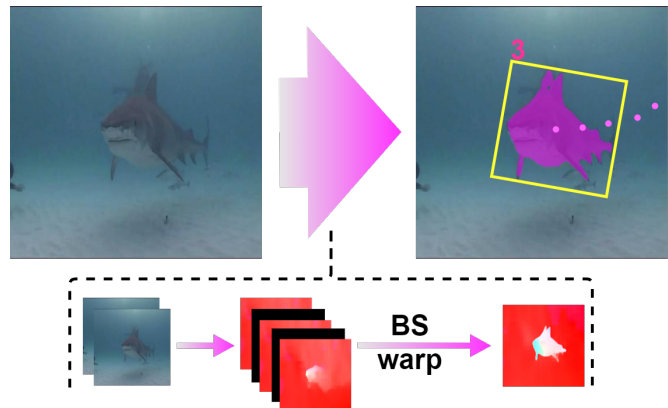


Fig. 1. Combining background subtraction and optical flow demonstrate how both levels work in concert to preserve object boundaries and temporal coherence throughout the video. Please refer to Sec. III for details.

This study was motivated by the importance of the challenges faced when trying to annotate and segment animals in videos in the wild. Unlike in controlled conditions, where animals are easily distinguishable from the background, fish are difficult to distinguish in realistic videos [18, 19], even with domain knowledge. This is due to large variations in animal appearance, lighting conditions, and background.

Our approach aims to develop an unsupervised method for fish tracking and segmentation without the need for human annotations, by leveraging spatial and temporal variations in video data using known techniques of background subtraction and optical flow, as shown in Fig. 1. Specifically, we propose to generate pseudo labels based on unlabelled video data. The use of pseudo labels can benefit various learning-based algorithms since it can significantly reduce the labelling cost. The key to the proposed method is to leverage the intrinsic temporal consistency between consecutive frames to improve the generated labels by refining them with a self-supervised model. We propose to train a DNN to segment individual fish based on the generated pseudo-labels. As long as the pseudo-labels are generated in a way that they have similar structure and appearance to real ones, the model can learn to understand the underlying structure from the pseudo-labels. In general, the more realistic the pseudo-labels, the better the segmentation accuracy. We include a short video of our model’s prediction at <https://youtu.be/Z5G7YBoL3eM> and

<https://youtu.be/8LOKsVSiY9U>.

The main contributions of this paper are listed as follows:

- Propose to use pixel-level pseudo labels generated by an optical-flow model and background subtraction to learn the segmentation and tracking of individual fish automatically without manual interaction.
- Demonstrate that using self-supervised refinement, we can further improve the accuracy of the pseudo labels for fish tracking and segmentation.
- Evaluate our method on three public datasets with different image quality.
- Discuss the limitations of the current model and our future research directions.

The rest of the paper is organized as follows. Sec. II covers related works and provides background information on the novel aspects of our work. Our model’s framework is described in detail in Sec. III. Sec. IV presents our method for training and evaluating our model. The experimental setup and results are presented in Sec. V, while detailed discussions of our results are presented in Sec. VI. Finally, Sec. VII concludes our paper.

II. RELATED WORK

In this section, we briefly review the research domains most relevant to our work.

Video object segmentation is a task that is used to locate and segment each target object [20–22]. The target object to be segmented can either be a class of interest in the videos or the moving objects of interest. Object segmentation is generally categorized into two categories: segmentation with instance-level semantics and segmentation without instance-level semantics, which is the main objective of this paper. Therefore, this study focuses on generating labels without human intervention. Some segmentation methods for moving objects have been developed by using background subtraction techniques [23–25]. Several of these approaches are based on the assumption that the scene is locally constant [26, 27]. This means that the background in one frame is assumed to be similar to the background in the next frame or only a few pixels away. In order to use this assumption, they estimate the local background and threshold it according to the similarity threshold to identify foreground regions. However, this method is known to be sensitive to illumination changes, and may even lose all detail within the image due to over-estimating the local background. Another approach to segmentation uses the detection of optical flow to define motion boundaries [28–31].

Optical flow predicts the relative motion of objects in two consecutive frames of a video [30, 31]. It gives a dense correspondence between frames, but at the cost of being limited to rigid objects, and computation entangled. Additionally, optical flow can only work within scenes where the movement of the camera is significantly lower than the movement of the object [28, 29, 32]. This can be seen as a limitation, as the background subtraction method can be used in a wider range of applications. However, the key element of optical flow is that it can also be used for background subtraction [33, 34].

By tracking the movement of the pixels between frames, we can determine the background. If a pixel that is part of the background does not match the static background within a given threshold, then that pixel is determined to be an instance of an object.

Another segmentation approach is based on the detection of visual motion. It is based on the fact that moving objects in the scene induce consistent changes to the flow of pixels in a region [29, 32]. However, due to substantial displacements or occlusions, their calculated optical flow may contain considerable inaccuracies [35–37]. In our method, we address these issues and enhance both estimated optical flow and object segmentation, simultaneously.

Video object tracking is the task of assigning a consistent label for each individual object in the scene as it moves [38, 39]. This tracking is generally divided into multiple steps, including detection of the object of interest, tracking of the moving object in the scene, and then associating labels between frames. The tracking task, therefore, consists of identifying the bounding box of the object over several video frames and, at the same time, updating the location of the object in the image [40, 41]. This can be done based on a similarity metric between different frames [42, 43]. The idea of such a metric is to find the closest objects in the frame with an overlapping bounding box. This can be performed at either the pixel level or at the region level. The major drawback of this method is the computation time [44, 45] that is needed to compute all the similarities between all the different frames. On the other hand, if the computational resources are available, this method has been proven to be useful when tracking fast-moving objects and when the objects are not occluded in the frame [46, 47]. In our method, we produce the rotating 2D object bounding box from each instance mask of the object over several video frames.

Supervised And Unsupervised Learning. Supervised learning has been used to build object detection [48–50], video object segmentation [21, 22] and video object tracking [39, 40]. These methods require extensive human annotation and therefore are not suitable for video annotation in the wild. To reduce the labelling costs of data, unsupervised learning has emerged as a powerful technique for the learning of video data. In the traditional image domain, unsupervised methods are expected to outperform their supervised counterparts [10, 11, 13, 51, 52] due to their potential to train data without labels.

The idea behind many of the unsupervised DNN models is to learn a feature representation from unlabelled data [53–55]. Then, a DNN model can be applied to the learned feature representation to produce the output. For example, in the domain of video segmentation [12, 56–58], DNNs have been used to learn a representation from the difference between a pair of unlabelled videos [59–61] and from warped frames [62].

In this work, we focus on unsupervised learning. Our proposed method will generate labels referred to as pseudo-labels to train a multi-task supervised DNN for video object segmentation and video object tracking.

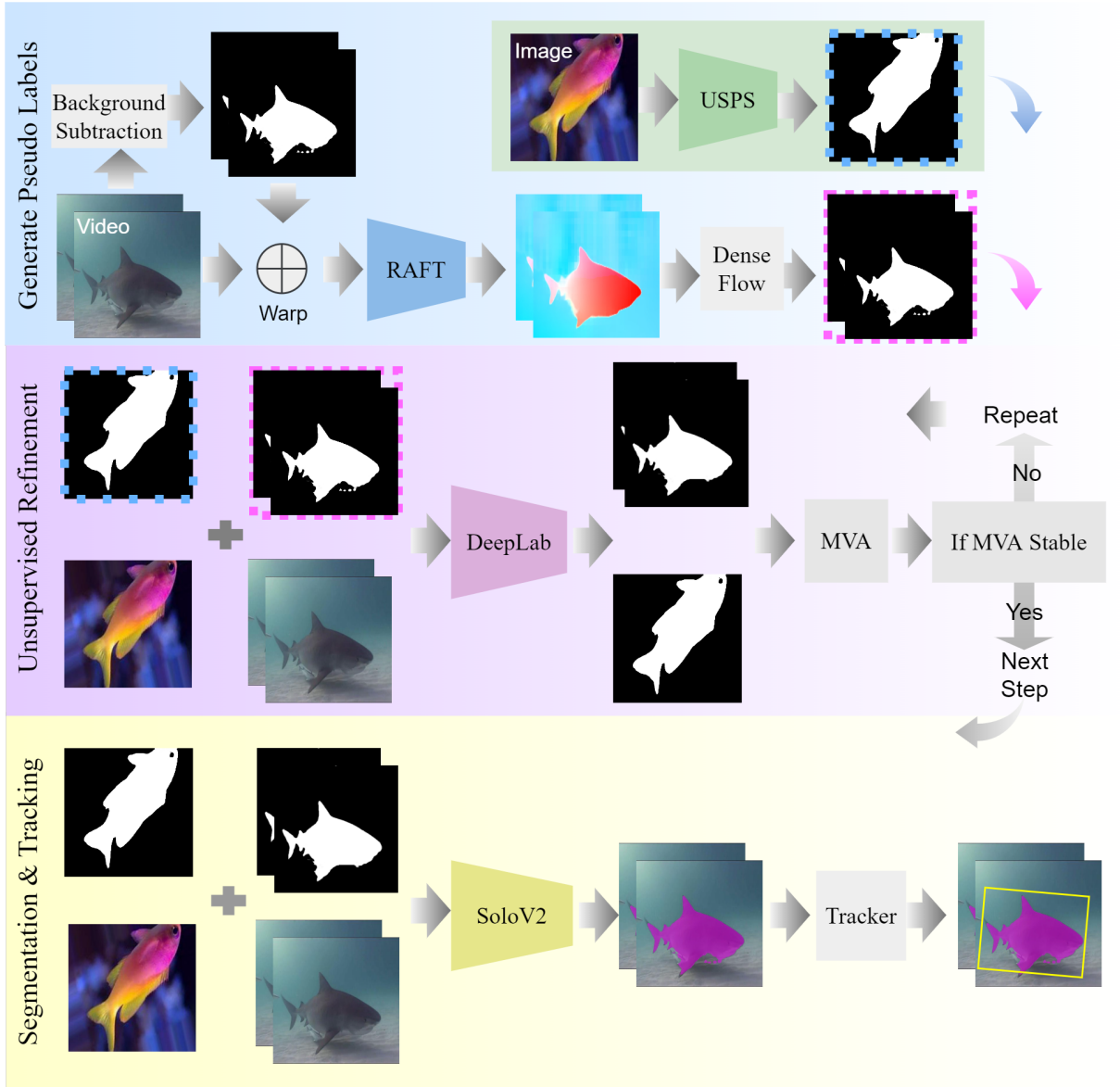


Fig. 2. Our proposed framework consists of three main components: generate pseudo-labels, unsupervised pseudo-labels refinement, and segmentation network. The top right panel in the pseudo label generation step is for generating pseudo labels from static images (not videos), as explained in Sec. IV-B. The proposed segmentation model trains with the generated pseudo-labels, which are refined with self-supervised training. Please refer to Sec. III for details.

III. FRAMEWORK

The overall framework can be divided into three stages as shown in Fig. 2. The first stage is to generate pseudo-labels using background subtraction and optical flow for both videos and still images. The second stage is to train a self-supervised model to refine the pseudo-labels using their spatial structure. In the last stage, the refinement of the video and still-image versions are applied jointly to train the segmentation network and to predict the final label. The segmentation network’s training behavior closely matches supervised training because we employ improved pseudo-labels. As a result, the network’s training process is more reliable than that of current unsupervised learning techniques [59–61, 63]. In the following subsections, we describe the details of these three components and the corresponding loss functions.

A. Background Subtraction

As a first step to generating pseudo labels, background subtraction is performed on the video frames. A clean background image is estimated for every video sequence by computing the median of the first 10 frames of the video sequence along the first axis. This is to average out any distracting elements that come in front of the clean background. Then, each video frame is subtracted from the clean background to create the mask sequence. After the subtraction, all the foreground pixels take on a value of 1, and pixels belonging to any background region have 0 values using Adaptive Gaussian Thresholding [64].

Adaptive Gaussian Thresholding is used instead of one global value as a threshold because it sets a pixel’s threshold based on a local region surrounding it. As a consequence, we obtain various thresholds for various areas inside the same

image, which produces better results for images with varying illumination.

This background subtraction step is crucial in eliminating any stationary elements or shadows from the video sequences that might disturb the next step, optical flow.

B. Optical Flow

The next step of pseudo-label generation is to compute the optical flow using Recurrent All-Pairs Field Transforms (RAFT) [65]. However, optical flow is frequently inaccurate at object boundaries, in which we want our segmentation to be accurate exactly at these borders. Therefore, we consider video segmentation from background subtraction and optical flow estimation simultaneously. Using pixel level and temporal information sources, the segmentation algorithm is improved by removing the artifacts induced by background subtraction and optical flow. We demonstrate how both levels work in concert to preserve object boundaries and temporal coherence throughout the video. The key is that we need to remove motion blurs while preserving the motion of the fish boundaries.

To achieve the pseudo labels, we first deconstruct a pair of video frames, x_t and x_{t+1} , and estimate a mask m_t and m_{t+1} with the background subtraction method as described in section Sec. III-A. The segmented masks m_t , m_{t+1} are used to synthesize frames \hat{x}_t and \hat{x}_{t+1} by warping x_t and x_{t+1} with m_t , m_{t+1} , respectively. The optical flow [65] takes two frames \hat{x}_t and \hat{x}_{t+1} , and produces a motion vector \hat{v} between them. This motion vector is used to compute the magnitude and angle of the motion. Specifically, the pixels with a motion vector \hat{v} outside m_t (and m_{t+1}) are assigned the value of the background and the pixels with a motion vector \hat{v} inside m_t (and m_{t+1}) are reassigned the object. We denote the reassigned images as \hat{x}_t^* and \hat{x}_{t+1}^* and use them as input for our segmentation step, as shown in the top panel of Fig. 2.

We show the optical flow results for the three video datasets with and without background subtraction of frames x_t and x_{t+1} in Fig. 4, Fig. 5, and Fig. 6. A mask m_{t+1} that better distinguishes the background from the foreground from the optical flow step is then refined with our proposed unsupervised refinement method in the next section. A sample optical flow comparison video before and after background subtraction is available at <https://youtu.be/8LOksVSiy9U>.

C. Unsupervised Refinement

The second stage in our method is cumulative pseudo-label refining via unsupervised historical moving averages (MVA) [68] using DeepLabv3 [69] network for semantic segmentation and Conditional Random Fields (CRF) [70] by minimizing the F-score until the MVA predictions reach a stable state. The CRF can "sharpen" initial location predictions to make them more accurate and consistent with edges and parts of the source image that have a constant colour.

Given the pseudo-labels of the previous step, we train the network for 50 epochs. The number of epochs is low to avoid a significant over-fitting of the network to the noisy pseudo-labels. Then, the network is reinitialized with trained weight to predict a new set of pseudo-labels to train on again.

Let D be the set of training examples and M be the network model. By $M(x, p)$ we denote the mask prediction of model M over pixel p of image $x \in D$. During this stage, a historical moving average (MVA) from the last training stage is composed as follows:

$$\text{MVA}(x, p, k) = (1-\alpha) * \text{CRF}(M(x, p)) + \alpha * \text{MVA}(x, p, k-1),$$

where $M(x, p)$ is the network mask prediction, k is the epoch number, α is a positive real factor, and CRF is the Conditional Random Fields (CRF) [70].

We use $L_\beta = 1 - F_\beta$ as an *image-level loss* function w.r.t. each training example x . F-score (F_β) is the harmonic mean of precision and recall of the prediction output of pixel p over image x w.r.t. the pseudo-labels, that use a positive real factor β as follows:

$$F_\beta = (1 + \beta^2) \frac{\text{precision} \cdot \text{recall}}{\beta^2 \text{precision} + \text{recall}}.$$

The network is retrained until the MVA reaches a stable state, as shown in the middle panel of Fig. 2. By doing so, the quality of pseudo-labels is improved over time.

D. Segmenting Objects by Locations

Our last stage is training a supervised segmentation model using the refined pseudo-labels from the previous stage. The supervised model is based on Segmenting Objects by Locations (SoloV2) [71]. SoloV2 is an updated version of Solo [72], a previous method for instance segmentation. The idea is to dynamically segment objects by location.

Given an image as input, the network generates the object mask, then the object mask generation is decoupled into a mask kernel prediction and mask feature learning. Furthermore, matrix non-maximum suppression (MNMS) is applied to reduce inference overhead. Specifically, SoloV2 is composed of two modules: (1) Dynamic Instance Segmentation and (2) Matrix non-maximum suppression (MNMS). The dynamic instance segmentation scheme dynamically segments objects by locations by learning the mask kernels and mask features separately. The mask kernels are predicted dynamically by the Fully Convolutional Network (FCN) [73] when classifying the pixels into different location categories, then constructing a unified mask feature representation for instance-aware segmentation. The non-maximum suppression process is achieved by performing NMS with a parallel matrix operation in one shot to reduce inference overhead and suppress duplicate predictions. Compared to the widely adopted multi-class NMS [74], where the sequential and recursive operations result in non-negligible latency, the parallel non-maximum suppression with matrix operation can achieve similar performance with much lower latency. The parallel processing strategy performs the inference for the MNMS on-the-fly and enables processing at a high frame rate (34 frames per second). For more details, we refer the readers to [71].

E. Rotating Bounding-box

From each instance mask that we predicted from the previous stage, we are able to produce the rotating 2D object bounding box. The minimum bounding rectangle (MBR) technique



Fig. 3. Sample image from each of the four utilised datasets. From left: Seagrass [18], DeepFish [19], YouTube-VOS [66], and Mediterranean Fish Species [67]

is used to obtain a rotated bounding box from a binary mask of the object. We used OpenCV [75] to find the minimum area of a rotated rectangle. It takes the binary mask of the object as an input and returns a Box2D structure that contains the following information: (centre (x, y) , (width, height), angle of rotation). The output of this step is used to track the objects as discussed in the following section.

F. Online Tracking

We used Simple Online and Real-Time Tracking (SORT) [76] as an online tracking framework that focuses on frame-to-frame prediction and association. The bounding box position and size are only used for both motion estimation and data association. Kalman filter [77] is used to handle the motion estimation and the Hungarian method [78] is used for data association.

Motion estimation is used to propagate a targets identity into the next frame. The inter-frame displacements of each object are approximated with a linear constant velocity estimation. The detected bounding box is used to update the target state where the Kalman filter [77] solves the velocity components. The state of each target is estimated as:

$$x = [h, v, s, r, \hat{h}, \hat{v}, \hat{s}]^T,$$

where h and v represent the horizontal and vertical pixel location of the center of the target, while s and r represent the scale and the aspect ratio of the targets bounding box, respectively. Here, $\hat{h}, \hat{v}, \hat{s}$ are for the source.

Data association is assigning new detections to existing targets. Each targets bounding box is estimated by predicting its new location in the current frame. The intersection-over-union (IOU) distance between each detection and each forecasted bounding box from the existing targets is used to calculate the assignment cost matrix. The assignment cost matrix is then resolved using the Hungarian technique [78] to produce the fish trajectory as shown in Fig. 7.

IV. METHOD

This section describes our method in detail. Our method is based on three main components: the pseudo labels generation, the unsupervised learning method to refine the generated pseudo labels and the DNN for fish tracking and segmentation. Fig. 2 shows the algorithm flow diagram for the fish tracking and segmentation framework.

A. Datasets

We performed experiments using four publicly available datasets, i.e. Seagrass [18], DeepFish [19], YouTube-VOS [66], and Mediterranean Fish Species [67]. Fig. 3 demonstrates a sample image from each dataset.

Seagrass [18] is comprised of annotated footage of *Girella tricuspidata* in two estuary systems in south-east Queensland, Australia. The raw data was obtained using submerged action cameras (HD 1080p). The dataset includes 4280 video frames and 9429 annotations. Each annotation includes segmentation masks that outline the species as a polygon.

DeepFish [19] consists of a large number of videos collected from 20 different habitats in remote coastal marine environments of tropical Australia. The video clips were captured in full HD resolution (1920×1080 pixels) using a digital camera. In total, the number of video frames taken is about $40k$.

YouTube-VOS [66] is a video object segmentation dataset that contains 4453 YouTube video clips and 94 object categories. The videos have pixel-level ground truth annotations for every 5th frame ($6fps$). For a fair comparison, we extracted only the videos that contained fish, which include 130 video clips and 4349 video frames in total.

Mediterranean Fish Species [67] consists of a large number of images collected from 20 different Mediterranean fish species. In total, the number of images is about $40k$. The dataset was split into two subfolders, training and test sets. The training set contains $34k$ and the test set contains $6k$ images. The image resolution ranges between (220×210 pixels) and (1920×1080 pixels). The original images are stored in an RGB file format in subfolders as a class label.

We train our feature extractor on all of the four datasets and evaluate it on the video datasets only, Seagrass [18], DeepFish [19], and YouTube-VOS [66].

B. Pseudo Labeling

To train our supervised model, which was explained in Sec. III-D, we first generate pseudo labels for the image dataset, Mediterranean Fish Species [67] and the video datasets, Seagrass [18], DeepFish [19], and YouTube-VOS [66].

1) *Image Dataset*: Since our image dataset [67] is curated from static images of different fish species, our framework discussed in Sec. III was not applicable to this dataset. Therefore, we used DeepUSPS [68] as an unsupervised saliency prediction network for a pseudo-labels generation. DeepUSPS

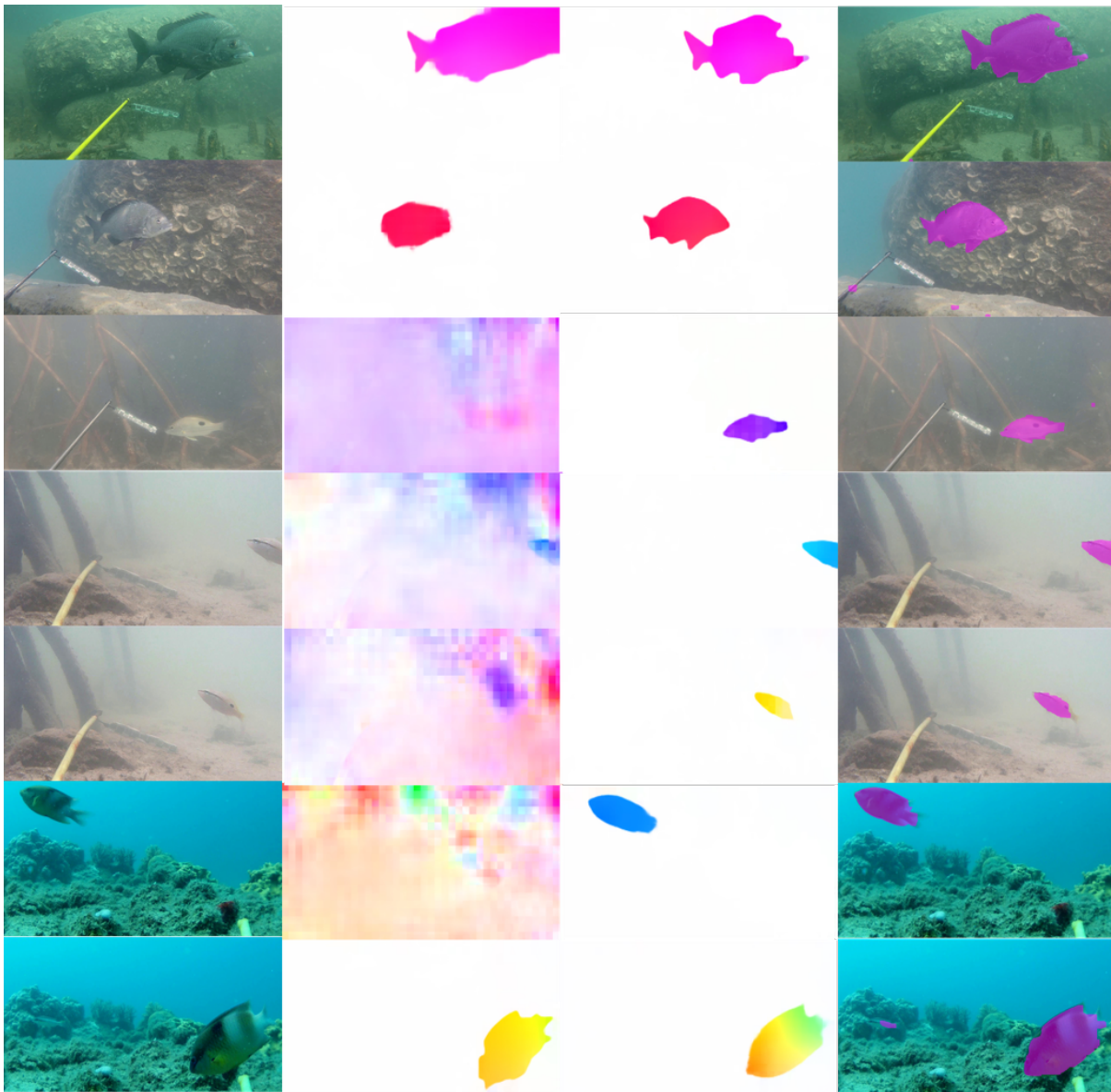


Fig. 4. Sample optical flow results for Seagrass [18]. From left, the original image, optical flow without background subtraction, optical flow with background subtraction, mask overlay.

is trained on the unlabelled MSRA-B dataset [79] for predicting salient objects. And it is an unsupervised learning method that produces pseudo labels with high intra-class variations, which is useful for the training of the supervised model.

However, DeepUSPS is only good in pseudo prediction for a single object in the image that is not disturbed by additional intricate details, which is not ideal for the more challenging video datasets [18, 19, 66].

2) *Video Datasets*: Unlike our image dataset, our video datasets contain both multiple objects in a single frame as well as across multiple frames. Therefore, we adapted our pseudo-label generation framework discussed in Sec. III that is capable of predicting multiple salient objects in the same video clip and handling the case of a cluttered background. This pseudo-label generation framework aims to tackle the issue of single-image datasets by generating more pseudo labels with

intra-class variations in image space.

The Pseudo-label generation framework consists of three steps:

- 1) Obtain salient objects by performing background subtraction using Adaptive Gaussian Thresholding [64], as explained in Sec. III-A.
- 2) Enhance the obtained salient object boundaries from the previous step with optical flow using RAFT [65], as explained in Sec. III-B.
- 3) Apply cumulative pseudo-label refining via unsupervised historical moving averages (MVA) [68], as explained in Sec. III-C.

In this way, we can get pseudo labels for video datasets, Seagrass [18], DeepFish [19], and YouTube-VOS [66], which are used to train the supervised model.

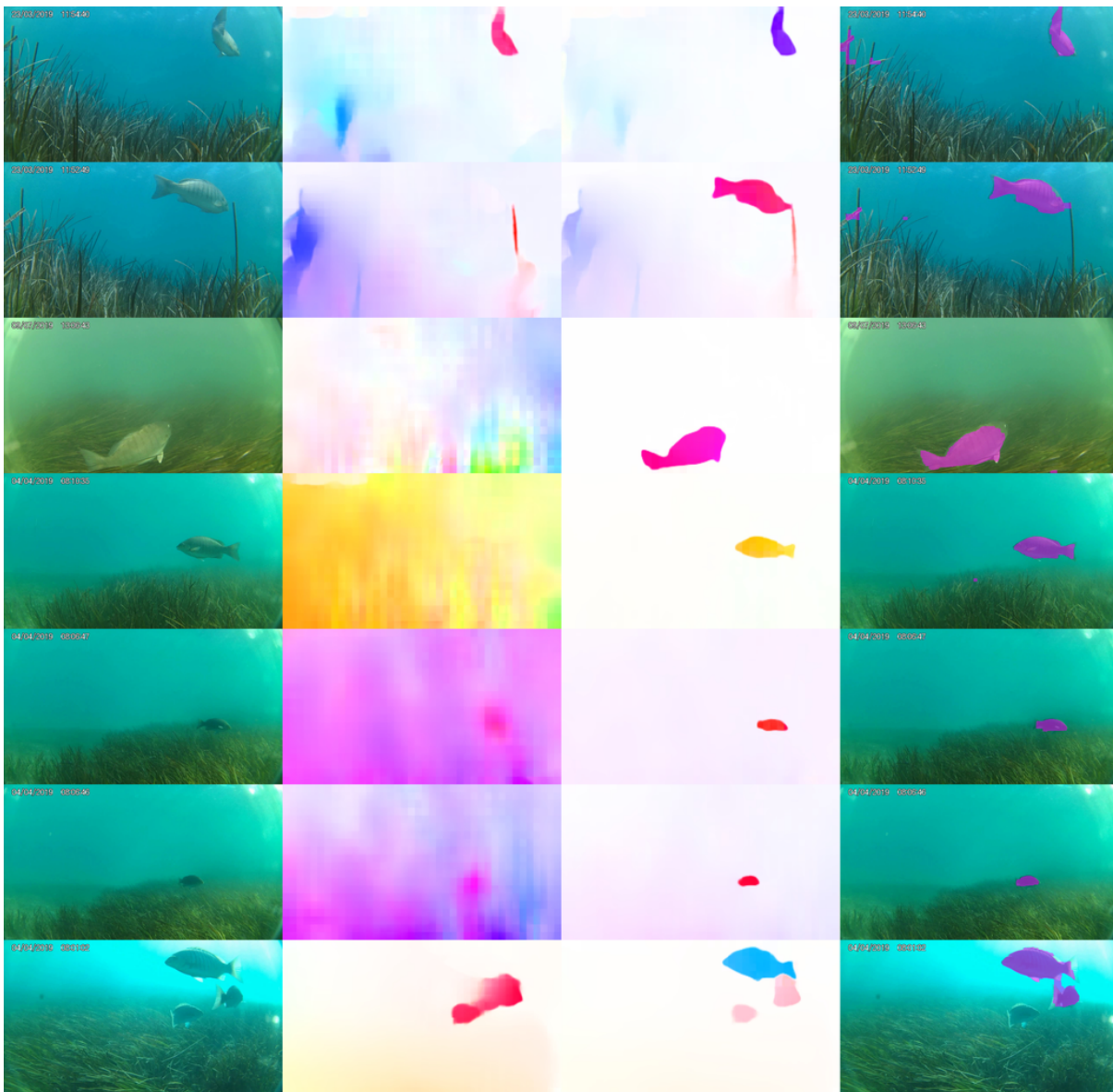


Fig. 5. Sample optical flow results for DeepFish [19]. From left, the original image, optical flow without background subtraction, optical flow with background subtraction, mask overlay.

C. Model training

Our models were trained with an input resolution of 256×256 pixels. We scale the lowest side of the video frames to 256 and then extract random crops of size 256×256 . We sample two video sets, $B = 2$ (of size $T = 5$ frames), therefore, $B \times T = 2 \times 5 = 10$ frames are used per forward pass.

We found that for this problem set, a learning rate of 1×10^{-3} works the best. It took around 300 epochs for all models to train on this problem. Our networks were trained on a Linux host with a single NVidia GeForce RTX 2080 Ti GPU with 11 GB of memory, using Pytorch framework [80]. We used stochastic gradient descent (SGD) optimiser [81] with an initial learning rate of 0.01, which is then divided by 10 at 27th and again at 33th epoch. We use light augmentation (resizing, grayscale). Following [71, 82], a scale jitter is used, where the shorter image side is randomly sampled from 640

to 800 pixels.

We applied the same hyperparameter configuration for all of the models. However, the optimum model configuration will depend on the application, hence, these results are not intended to represent a complete search of model configurations.

D. Inference

During tracking, we extract frames from the input video, forward each frame through the network, and obtain the fish category score from the classification branch. Initially, to filter out predictions with low confidence, we use a threshold of 0.1 and perform convolution on the mask feature using corresponding predicted mask kernels. Then, after having applied a per-pixel sigmoid, we binarise the output of the mask branch at the threshold of 0.5. The final step is the Matrix NMS, which fits the output mask with the Min-max box.

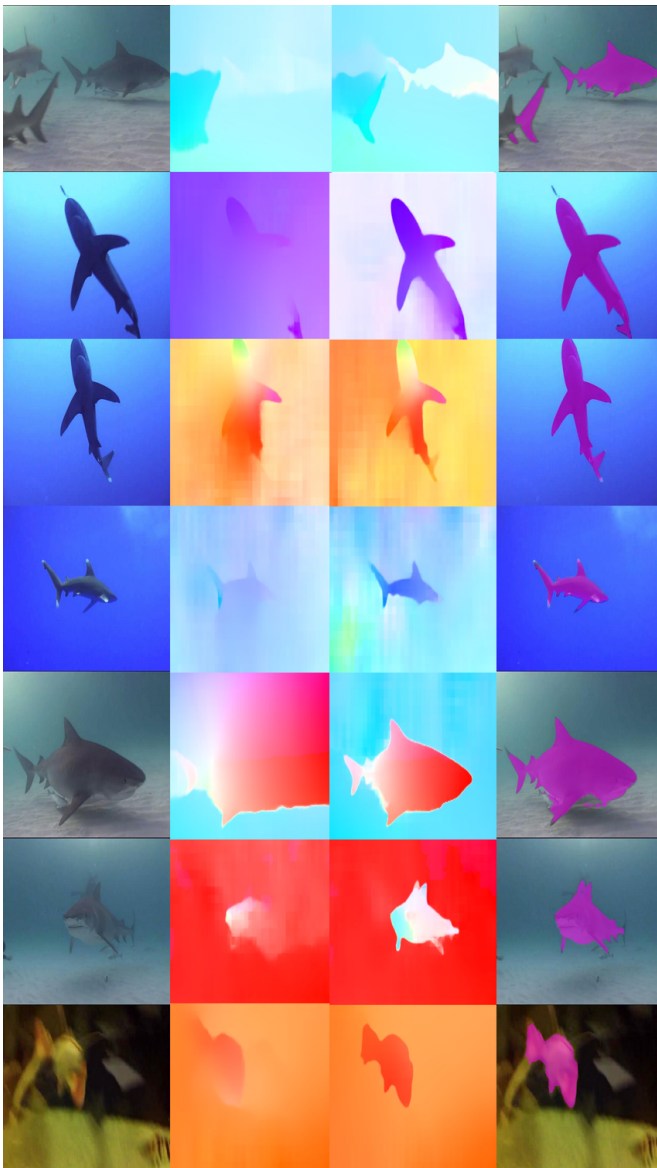


Fig. 6. Sample optical flow results for YouTube-VOS [66]. From left, the original image, optical flow without background subtraction, optical flow with background subtraction, mask overlay.

Our model operates online without any adaptation to the video sequence. On a single NVidia GeForce RTX 2080 Ti GPU, we measured an average speed of 34 frames per second.

V. EXPERIMENTS

We report experimental results for our model’s trained representation on 50% of the DeepFish, Seagrass, YouTube-VOS datasets and the train set of the Mediterranean Fish Species dataset. We then evaluate it on the other 50% of the first three datasets. We provide quantitative and qualitative results that demonstrate our model’s generalization capabilities to a range of different underwater habitats.

A. Results

We summarize our main results on Seagrass [18], DeepFish [19] and YouTube-VOS [66] datasets in Table I. The quanti-

tative results for all datasets were obtained using the COCO dataset [83] evaluation script. The average precision (AP), the average recall (AR), and Intersection over Union (IoU) were measured for the predicted bounding boxes and segmentation masks in the output images obtained from the trained SoloV2 [71], as explained in Sec. III-D in detail.

The $AP^{.50}$ and $AP^{.75}$ values were measured with the IoU thresholds of 0.5 and 0.75, respectively. The AP^M and AR^M values show the average of the AP and AR values for 10 IoU thresholds of .50 : .05 : .95, respectively. Averaging over $IoUs$ rewards detectors with better localization. The AP^L and AR^L values show the AP and AR values over a large area ($> 96^2$). This area is measured as the number of *pixels* in the segmentation mask. We observed that the performance of the proposed model is stable across these three datasets. This validates the proposed model’s ability to generalize well to unseen videos in other environments.

To the best of our knowledge, there is no previous work reporting detection and segmentation evaluation for these datasets. To compare our proposed unsupervised method to a supervised approach, SoloV2 [71] results on the three datasets are reported with the authors’ implementation in Table II. This Table shows the results of a fully supervised model with the original labels, not our generated pseudo-label.

The close accuracy results of our proposed unsupervised method compared to the original supervised SoloV2 [71] in both the detection and segmentation experiments, validate our generative approach. Moreover, our results indicate that the proposed model is not heavily influenced by different underwater habitats. The performance is on par for DeepFish [19] and Seagrass [18]. Seagrass [18] is relatively challenging since the fish are not as easy to visually detect as in the other datasets. In some cases, the proposed model is not as good as the fully supervised approaches. However, the main purpose of this study is to develop an unsupervised method for fish tracking and segmentation. We believe that our proposed approach is more stable during training than other unsupervised methods that do not include a dedicated pseudo-label generation step.

TABLE I

COMPARISON OF *UNSUPERVISED* DETECTION AND SEGMENTATION ON SEAGRASS [18], DEEPFISH [19] AND YOUTUBE-VOS [66] DATASETS.

Dataset	AP^M	$AP^{.50}$	$AP^{.75}$	AP^L	AR^M	AR^L
<i>Evaluating Detection:</i>						
Seagrass [18]	22.1	72.5	13.7	38.2	61.4	61.3
DeepFish [19]	11.7	35.0	05.3	19.3	34.5	57.1
YouTube-VOS [66]	23.6	43.2	18.4	26.9	46.1	57.5
<i>Evaluating Segmentation:</i>						
Seagrass [18]	12.0	37.6	05.2	20.8	31.2	52.0
DeepFish [19]	31.2	75.0	24.4	43.8	56.6	59.4
YouTube-VOS [66]	15.4	33.0	12.2	19.2	33.8	42.2

Qualitative results of our algorithm for DeepFish [19], Seagrass [18] and YouTube-VOS [66] datasets are shown in Fig. 8, Fig. 9 and Fig. 10, respectively. We also include additional examples of failure cases in Fig. 11. Overall, especially for non-rigid objects, the proposed algorithm produces



Fig. 7. Sample fish trajectory results. Zoom-in for better view. See also a short video of fish trajectory results at <https://youtu.be/Z5G7YBoL3eM>.

favourable outcomes in the majority of images. This is despite the fast movements or crowded and complicated backgrounds causing these images to frequently have significant distortion. See also a short video of our model’s prediction at <https://youtu.be/Z5G7YBoL3eM>.

TABLE II

COMPARISON OF *SUPERVISED* DETECTION AND SEGMENTATION ON SEAGRASS [18], DEEPFISH [19] AND YOUTUBE-VOS [66] DATASETS.

Dataset	AP^M	$AP^{.50}$	$AP^{.75}$	AP^L	AR^M	AR^L
<i>Evaluating Detection:</i>						
Seagrass [18]	32.4	82.2	13.0	34.9	68.5	72.4
DeepFish [19]	12.2	41.8	04.3	20.9	41.0	68.0
YouTube-VOS [66]	25.9	56.2	21.6	32.8	54.1	69.9
<i>Evaluating Segmentation:</i>						
Seagrass [18]	18.0	56.4	07.8	31.2	36.8	68.0
DeepFish [19]	46.8	72.5	36.6	50.7	64.9	72.1
YouTube-VOS [66]	23.1	49.5	18.3	28.8	40.7	53.3

B. Ablation Study

We performed an ablation study to demonstrate the proposed approach’s effectiveness in generating pseudo labels. Specifically, we analyzed the contribution of the vital component in the proposed method, the optical flow with background subtraction (Sec. III-B). In addition, we evaluated the segmentation network training with refined pseudo-labels (Sec. III-D) for different epochs. The results reported in Table III are for the unsupervised segmentation based on optical flow without background subtraction as a baseline. And the results reported in Table IV are for the four epochs trials with the same random seeds, please refer to Sec. IV-C for the details.

It is apparent from the results that the segmentation accuracy of our proposed method has improved significantly when compared to that of the baseline method. We also note that the accuracy of the models also depends on the number of epochs used in the training. We observe from the results shown in Table IV that the segmentation accuracy decreases after 100 epochs. The reason for this is the over-fitting of the network to

the noisy pseudo-labels. While the training losses for both the baseline and our model decreased, the segmentation accuracy for our model was still greater than that for the baseline.

TABLE III

COMPARISON OF *UNSUPERVISED* SEGMENTATION BASED ON OPTICAL FLOW *without* BACKGROUND SUBTRACTION.

Dataset	AP^M	$AP^{.50}$	$AP^{.75}$	AP^L	AR^M	AR^L
<i>Evaluating Segmentation:</i>						
Seagrass [18]	05.0	23.8	03.1	14.7	19.7	29.5
DeepFish [19]	15.3	44.8	13.6	33.5	42.7	37.4
YouTube-VOS [66]	07.2	23.8	07.4	11.9	26.1	33.0

TABLE IV

COMPARISON OF *UNSUPERVISED* SEGMENTATION FOR DIFFERENT EPOCHS: 50,100,150,300

Dataset	AP^M	$AP^{.50}$	$AP^{.75}$	AP^L	AR^M	AR^L
<i>50 epochs:</i>						
Seagrass [18]	12.4	33.6	07.2	20.4	28.4	47.2
DeepFish [19]	32.0	68.6	30.8	34.8	53.6	56.2
YouTube-VOS [66]	15.8	34.0	13.8	19.8	33.8	42.2
<i>100 epochs:</i>						
Seagrass [18]	12.0	37.6	05.2	20.8	31.2	52.0
DeepFish [19]	31.2	75.0	24.4	43.8	56.6	59.4
YouTube-VOS [66]	15.4	33.0	12.2	19.2	33.8	42.2
<i>150 epochs:</i>						
Seagrass [18]	12.0	36.0	04.8	20.4	30.0	48.8
DeepFish [19]	30.4	69.8	23.2	32.4	54.2	56.8
YouTube-VOS [66]	15.2	34.0	14.0	20.2	32.8	41.0
<i>300 epochs:</i>						
Seagrass [18]	10.8	33.6	04.0	18.8	28.0	46.4
DeepFish [19]	29.8	70.0	22.4	31.8	53.0	55.6
YouTube-VOS [66]	15.2	33.8	14.4	23.0	32.0	40.0

VI. DISCUSSION

Fish segmentation and tracking are notoriously difficult tasks, especially for small fish in video data where the

background, lighting conditions and fish shape can vary significantly. In particular, for real data, the quality of ground truth labels varies from video to video since it is difficult to annotate the animal’s entire path. Therefore, our model aims to generate a pseudo ground truth by leveraging temporal consistency between frames and improving its quality based on self-supervised learning. The key to our proposed model is to leverage the intrinsic temporal consistency between consecutive frames by using the optical flow and background subtraction method to improve the generated labels. This is especially important when the fish is moving quickly and not in the same location in the consecutive frames, as is the case in natural data. Tracking fish in video data is also challenging because their motion is very irregular and small fish may not be visible throughout the entire dataset. The other problem is that segmentation and tracking are time-consuming tasks, especially when dealing with large datasets.

Our model outperforms the baseline method (the optical flow without background subtraction) with higher AP values in most of the cases. Our approach can utilize temporal consistency to produce consistent labels. In the case of the DeepFish dataset [19], we observed that our proposed unsupervised model results in higher accuracy compared to the Seagrass dataset [18]. This is mainly due to the more challenging videos in the Seagrass dataset [18] compared to the video data in DeepFish [19]. Furthermore, we show that for different video datasets, our model shows similar accuracy. Therefore, we can expect that the accuracy would be similar when tested under the same conditions but in new underwater video datasets.

In addition, the segmentation accuracy does not degrade after training with supervised training, and training converges in only a few epochs, as shown in Table IV. In our experiments, we found that the segmentation quality has a significant impact on tracking performance. This is because the quality of the produced object bounding box has a high impact on tracking performance. Even in this case, we still achieved decent results.

We also analyzed the robustness of our proposed model with respect to the environmental conditions. We observed degradation of the model’s performance when several fish were heavily occluded, like in Fig. 11. However, our proposed model is still able to estimate the fish mask in some parts as long as they are part of the animal body. One of the main challenges in this task is the large variability in the size and shape of fish, as well as the variation in the shape of the fish’s body. While it is possible to identify a certain shape of fish, it is not always possible to determine the number of fish in the image.

Given a set of unlabeled video collections, the main limitation of our study is that it is only capable of segmenting foreground items and cannot distinguish between distinct object instances or semantic classes. Occasionally, the whole object or parts of the object may not be segmented out. Our model’s performance is highly influenced by the characteristics of training videos, the coverage of object categories, and the motion of both the camera and the objects, similar to other data-driven learning techniques. Our results are based on a few assumptions. One is that a small subset of semantically similar

objects (e.g., all fish) exists in the scene, and these objects are likely to share the same motion feature or to be semantically similar. These assumptions are reasonable if the objects are within a certain size range, they all belong to the same class, and most of them share similar colours, shapes, and sizes. Another limitation of our approach is that we used a relatively large number of videos with a relatively small number of object categories (for instance compared to ImageNet). This allows our model to segment objects of all shapes and colours with only a handful of training examples.

One other limitation of our current framework is that, in some cases, it is unable to detect all the objects that appear in the video. In future work, we intend to study how to develop a detection-based model that is able to detect all the objects appearing in a given scene. Therefore, in the next step, we should look for a more robust and generic objectness model that is able to generalize across a variety of object categories, and a variety of background types. Further work could be conducted on more fine-grained object segmentation, especially with new video datasets.

VII. CONCLUSION

We proposed a novel unsupervised method for tracking and segmenting fish in videos in the wild. Our results demonstrate that our proposed pseudo-label generation method that combines optical flow with background subtraction followed by an unsupervised refinement network, leads to accurate segmentation results when used to train a supervised segmentation DNN. We showed that this segmentation approach can be used for effective tracking. We tested our model on three challenging datasets with the results indicating that our method could be a valuable candidate for assisting in the video processing of fish behaviour. Future work can extend our approach to other animal species that are commonly found in aquatic environments. Another important direction is to extend this model to other fields, for example, tracking-by-detection for autonomous driving.

ACKNOWLEDGEMENT

This research is supported by the Australian Research Training Program (RTP) Scholarship and Food Agility HDR Top-Up Scholarship. D. Jerry and M. Rahimi Azghadi acknowledge the Australian Research Council through their Industrial Transformation Research Hub program.



Fig. 8. Sample images from our model results for DeepFish [19], From left, the original image, the ground truth, the predicted image.

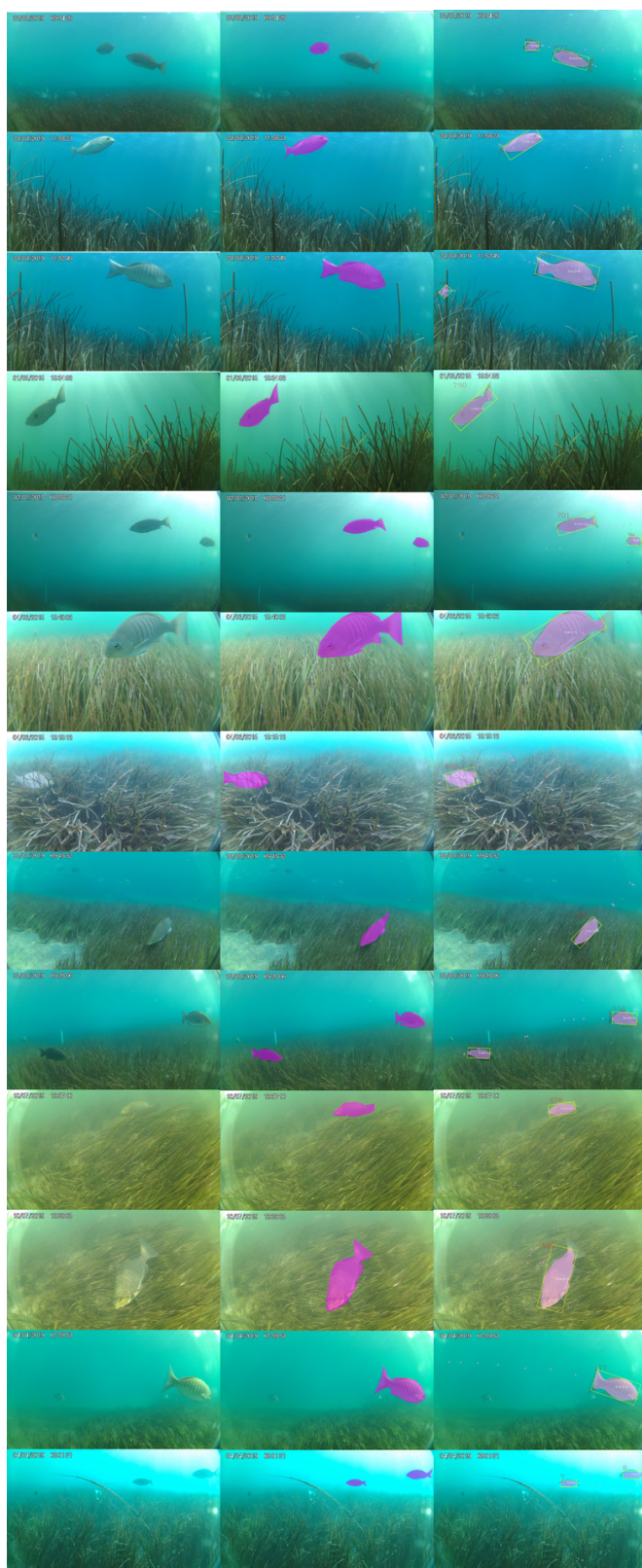


Fig. 9. Sample images from our model results for Seagrass [18], From left, the original image, the ground truth, the predicted image.



Fig. 10. Sample images from our model results for YouTube-VOS [66], From left, the original image, the ground truth, the predicted image.



Fig. 11. Sample images for failure cases, From left, the original image, the ground truth, the predicted image.

REFERENCES

- [1] S. LopezMarcano, E. Jinks, C. A. Buelow, C. J. Brown, D. Wang, B. Kusy, E. Ditria, and R. M. Connolly, "Automatic detection of fish and tracking of movement for ecology," *Ecology and Evolution*, vol. 11, no. 12, pp. 8254–8263, 6 2021. [Online]. Available: <https://onlinelibrary.wiley.com/doi/10.1002/ece3.7656>
- [2] L. Zou, M. Zhao, F. Cao, S. Zan, X. Cheng, and X. Liu, "Fish Tracking Based on Feature Fusion and Scale Adaptation in a Real-World Underwater Environment," *Marine Technology Society Journal*, vol. 55, no. 2, pp. 45–53, 3 2021. [Online]. Available: <https://www.ingentaconnect.com/content/10.4031/MTSJ.55.2.12>
- [3] P. Gatti, J. A. D. Fisher, F. Cyr, P. S. Galbraith, D. Robert, and A. Le Bris, "A review and tests of validation and sensitivity of geolocation models for marine fish tracking," *Fish and Fisheries*, vol. 22, no. 5, pp. 1041–1066, 9 2021. [Online]. Available: <https://onlinelibrary.wiley.com/doi/10.1111/faf.12568>
- [4] Y. Wageeh, H. E.-D. Mohamed, A. Fadl, O. Anas, N. ElMasry, A. Nabil, and A. Atia, "YOLO fish detection with Euclidean tracking in fish farms," *Journal of Ambient Intelligence and Humanized Computing*, vol. 12, no. 1, pp. 5–12, 1 2021. [Online]. Available: <http://link.springer.com/10.1007/s12652-020-02847-6>
- [5] A. Saleh, M. Sheaves, and M. Rahimi Azghadi, "Computer vision and deep learning for fish classification in underwater habitats: A survey," *Fish and Fisheries*, 4 2022. [Online]. Available: <https://onlinelibrary.wiley.com/doi/10.1111/faf.12666>
- [6] V. G. Guida, P. C. Valentine, and L. B. Gallea, "Semidiurnal Temperature Changes Caused by Tidal Front Movements in the Warm Season in Seabed Habitats on the Georges Bank Northern Margin and Their Ecological Implications," *PLoS ONE*, vol. 8, no. 2, p. e55273, 2 2013. [Online]. Available: <https://dx.plos.org/10.1371/journal.pone.0055273>
- [7] J. Sundin, R. Morgan, M. H. Finnøen, A. Dey, K. Sarkar, and F. Jutfelt, "On the Observation of Wild Zebrafish (*Danio rerio*) in India," *Zebrafish*, vol. 16, no. 6, pp. 546–553, 12 2019. [Online]. Available: <https://www.liebertpub.com/doi/10.1089/zeb.2019.1778>
- [8] E. M. Olsen, M. R. Heupel, C. A. Simpfendorfer, and E. Moland, "Harvest selection on Atlantic cod behavioral traits: implications for spatial management," *Ecology and Evolution*, vol. 2, no. 7, pp. 1549–1562, 7 2012. [Online]. Available: <https://onlinelibrary.wiley.com/doi/10.1002/ece3.244>
- [9] N. X. R. Wang, S. Cullis-Suzuki, and A. Branzan Albu, "Automated Analysis of Wild Fish Behavior in a Natural Habitat," in *Proceedings of the 2nd International Workshop on Environmental Multimedia Retrieval*. New York, NY, USA: ACM, 6 2015, pp. 21–26. [Online]. Available: <https://dl.acm.org/doi/10.1145/2764873.2764875>
- [10] A. Saleh, I. H. Laradji, D. A. Kononov, M. Bradley, D. Vazquez, and M. Sheaves, "A realistic fish-habitat dataset to evaluate algorithms for underwater visual analysis," *Scientific Reports*, vol. 10, no. 1, p. 14671, 12 2020. [Online]. Available: <http://www.nature.com>
- [11] D. A. Kononov, A. Saleh, D. B. Efremova, J. A. Domingos, and D. R. Jerry, "Automatic Weight Estimation of Harvested Fish from Images," in *2019 Digital Image Computing: Techniques and Applications, DICTA 2019*. Institute of Electrical and Electronics Engineers Inc., 12 2019.
- [12] I. H. Laradji, A. Saleh, P. Rodriguez, D. Nowrouzezahrai, M. R. Azghadi, and D. Vazquez, "Weakly supervised underwater fish segmentation using affinity LCFCN," *Scientific reports*, vol. 11, no. 1, p. 17379, 12 2021. [Online]. Available: <https://www.nature.com/articles/s41598-021-96610-2>
<http://www.ncbi.nlm.nih.gov/pubmed/34462458>
<http://www.pubmedcentral.nih.gov/articlerender.fcgi?artid=PMC8405733>
- [13] D. A. Kononov, A. Saleh, J. A. Domingos, R. D. White, and D. R. Jerry, "Estimating Mass of Harvested Asian Seabass *Lates calcarifer* from Images," *World Journal of Engineering and Technology*, vol. 6, no. 03, p. 15, 2018.
- [14] D. A. Kononov, A. Saleh, M. Bradley, M. Sankupellay, S. Marini, and M. Sheaves, "Underwater Fish Detection with Weak Multi-Domain Supervision," in *2019 International Joint Conference on Neural Networks (IJCNN)*, vol. 2019-July. IEEE, 7 2019, pp. 1–8. [Online]. Available: <https://ieeexplore.ieee.org/document/8851907/>
- [15] S. H. Wang, J. Zhao, X. Liu, Z.-M. Qian, Y. Liu, and Y. Q. Chen, "3D tracking swimming fish school with learned kinematic model using LSTM network," in *2017 IEEE International Conference on Acoustics, Speech and Signal Processing (ICASSP)*. IEEE, 3 2017, pp. 1068–1072. [Online]. Available: <http://ieeexplore.ieee.org/document/7952320/>
- [16] S. Villon, D. Mouillot, M. Chaumont, E. S. Darling, G. Subsol, T. Claverie, and S. Villéger, "A Deep learning method for accurate and fast identification of coral reef fishes in underwater images," *Ecological Informatics*, 2018.
- [17] Z. Li, W. Li, F. Li, and M. Yuan, "A Review of Computer Vision Technologies for Fish Tracking," *IEEE*, 10 2021. [Online]. Available: <http://arxiv.org/abs/2110.02551>
- [18] E. M. Ditria, R. M. Connolly, E. L. Jinks, and S. Lopez-Marcano, "Annotated Video Footage for Automated Identification and Counting of Fish in Unconstrained Seagrass Habitats," *Frontiers in Marine Science*, vol. 8, 3 2021. [Online]. Available: <https://www.frontiersin.org/articles/10.3389/fmars.2021.629485/full>
- [19] A. Saleh, I. H. Laradji, D. A. Kononov, M. Bradley, D. Vazquez, and M. Sheaves, "A realistic fish-habitat dataset to evaluate algorithms for underwater visual analysis," *Scientific Reports*, vol. 10, no. 1, p. 14671, 12 2020. [Online]. Available: <http://www.nature.com>

- articles/s41598-020-71639-x
- [20] R. Yao, G. Lin, S. Xia, J. Zhao, and Y. Zhou, "Video Object Segmentation and Tracking," *ACM Transactions on Intelligent Systems and Technology*, vol. 11, no. 4, pp. 1–47, 8 2020. [Online]. Available: <https://dl.acm.org/doi/10.1145/3391743>
- [21] A. Khoreva, R. Benenson, E. Ilg, T. Brox, and B. Schiele, "Lucid Data Dreaming for Video Object Segmentation," *International Journal of Computer Vision*, vol. 127, no. 9, pp. 1175–1197, 9 2019. [Online]. Available: <http://link.springer.com/10.1007/s11263-019-01164-6>
- [22] K.-K. Maninis, S. Caelles, Y. Chen, J. Pont-Tuset, L. Leal-Taixe, D. Cremers, and L. Van Gool, "Video Object Segmentation without Temporal Information," *IEEE Transactions on Pattern Analysis and Machine Intelligence*, vol. 41, no. 6, pp. 1515–1530, 6 2019. [Online]. Available: <https://ieeexplore.ieee.org/document/8362936/>
- [23] T. Bouwmans, S. Javed, M. Sultana, and S. K. Jung, "Deep neural network concepts for background subtraction: A systematic review and comparative evaluation," *Neural Networks*, vol. 117, pp. 8–66, 9 2019. [Online]. Available: <https://linkinghub.elsevier.com/retrieve/pii/S0893608019301303>
- [24] R. Kalsotra and S. Arora, "A Comprehensive Survey of Video Datasets for Background Subtraction," *IEEE Access*, vol. 7, pp. 59 143–59 171, 2019. [Online]. Available: <https://ieeexplore.ieee.org/document/8706931/>
- [25] B. Garcia-Garcia, T. Bouwmans, and A. J. Rosales Silva, "Background subtraction in real applications: Challenges, current models and future directions," *Computer Science Review*, vol. 35, p. 100204, 2 2020. [Online]. Available: <https://linkinghub.elsevier.com/retrieve/pii/S1574013718303101>
- [26] H. Pan, G. Zhu, C. Peng, and Q. Xiao, "Background subtraction for night videos," *PeerJ Computer Science*, vol. 7, p. e592, 6 2021. [Online]. Available: <https://peerj.com/articles/cs-592>
- [27] L. Maddalena and A. Petrosino, "Background Subtraction for Moving Object Detection in RGBD Data: A Survey," *Journal of Imaging*, vol. 4, no. 5, p. 71, 5 2018. [Online]. Available: <http://www.mdpi.com/2313-433X/4/5/71>
- [28] S. Lu, Z. Luo, F. Gao, M. Liu, K. Chang, and C. Piao, "A Fast and Robust Lane Detection Method Based on Semantic Segmentation and Optical Flow Estimation," *Sensors*, vol. 21, no. 2, p. 400, 1 2021. [Online]. Available: <https://www.mdpi.com/1424-8220/21/2/400>
- [29] S. Anthwal and D. Ganotra, "An overview of optical flow-based approaches for motion segmentation," *The Imaging Science Journal*, vol. 67, no. 5, pp. 284–294, 7 2019. [Online]. Available: <https://www.tandfonline.com/doi/full/10.1080/13682199.2019.1641316>
- [30] J. Cheng, Y.-H. Tsai, S. Wang, and M.-H. Yang, "SegFlow: Joint Learning for Video Object Segmentation and Optical Flow," in *2017 IEEE International Conference on Computer Vision (ICCV)*, vol. 2017-October. IEEE, 10 2017, pp. 686–695. [Online]. Available: <http://ieeexplore.ieee.org/document/8237343/>
- [31] M. Ding, Z. Wang, B. Zhou, J. Shi, Z. Lu, and P. Luo, "Every Frame Counts: Joint Learning of Video Segmentation and Optical Flow," *Proceedings of the AAAI Conference on Artificial Intelligence*, vol. 34, no. 07, pp. 10 713–10 720, 4 2020. [Online]. Available: <https://aaai.org/ojs/index.php/AAAI/article/view/6699>
- [32] A. Garcia-Dopico, J. L. Pedraza, M. Nieto, A. Pérez, S. Rodríguez, and L. Osendi, "Locating moving objects in car-driving sequences," *EURASIP Journal on Image and Video Processing*, vol. 2014, no. 1, p. 24, 12 2014. [Online]. Available: <https://jivp-urasipjournals.springeropen.com/articles/10.1186/1687-5281-2014-24>
- [33] S. Chraa Mesbahi, M. A. Mahraz, J. Riffi, and H. Tairi, "Head Gesture Recognition Using Optical Flow Based Background Subtraction," in *Lecture Notes in Networks and Systems*, 2018, vol. 37, pp. 200–211. [Online]. Available: http://link.springer.com/10.1007/978-3-319-74500-8_18
- [34] A. Kushwaha, A. Khare, O. Prakash, and M. Khare, "Dense optical flow based background subtraction technique for object segmentation in moving camera environment," *IET Image Processing*, vol. 14, no. 14, pp. 3393–3404, 12 2020. [Online]. Available: <https://onlinelibrary.wiley.com/doi/10.1049/iet-ipr.2019.0960>
- [35] D. Sun, C. Liu, and H. Pfister, "Local layering for joint motion estimation and occlusion detection," in *Proceedings of the IEEE Computer Society Conference on Computer Vision and Pattern Recognition*, 2014.
- [36] Z. Chen, H. Jin, Z. Lin, S. Cohen, and Y. Wu, "Large displacement optical flow from nearest neighbor fields," in *Proceedings of the IEEE Computer Society Conference on Computer Vision and Pattern Recognition*, 2013.
- [37] T. Brox and J. Malik, "Large Displacement Optical Flow: Descriptor Matching in Variational Motion Estimation," *IEEE Transactions on Pattern Analysis and Machine Intelligence*, vol. 33, no. 3, pp. 500–513, 3 2011. [Online]. Available: <http://ieeexplore.ieee.org/document/5551149/>
- [38] H. Guan, X. Y. Xue, and Z. Y. An, "Advances on application of deep learning for video object tracking," 2016.
- [39] G. Ciaparrone, F. Luque Sánchez, S. Tabik, L. Troiano, R. Tagliaferri, and F. Herrera, "Deep learning in video multi-object tracking: A survey," *Neurocomputing*, vol. 381, pp. 61–88, 3 2020. [Online]. Available: <https://linkinghub.elsevier.com/retrieve/pii/S0925231219315966>
- [40] R. Gomez-Nieto, J. F. Ruiz-Munoz, J. Beron, C. A. A. Franco, H. D. Benitez-Restrepo, and A. C. Bovik, "Quality Aware Features for Performance Prediction and Time Reduction in Video Object Tracking," *IEEE Access*, vol. 10, pp. 13 290–13 310, 2022. [Online]. Available: <https://ieeexplore.ieee.org/document/9698081/>
- [41] J. Qiu, L. Wang, Y. H. Hu, and Y. Wang, "Two motion models for improving video object tracking performance," *Computer Vision and Image Understanding*, vol. 195, p. 102951, 6 2020. [Online]. Available: <https://linkinghub.elsevier.com/>

- [retrieve/pii/S1077314220300345](https://www.mdpi.com/10.1007/s11042-020-09164-2)
- [42] X. Kang, B. Song, and F. Sun, “A Deep Similarity Metric Method Based on Incomplete Data for Traffic Anomaly Detection in IoT,” *Applied Sciences*, vol. 9, no. 1, p. 135, 1 2019. [Online]. Available: <https://www.mdpi.com/2076-3417/9/1/135>
- [43] A. Dadgar, Y. Baleghi, and M. Ezoji, “Improved Object Matching in Multi-Objects Tracking Based On Zernike Moments and Combination of Multiple Similarity Metrics,” *International Journal of Engineering*, vol. 34, no. 6, 6 2021. [Online]. Available: http://www.ije.ir/article_130893.html
- [44] S. Bag, S. K. Kumar, and M. K. Tiwari, “An efficient recommendation generation using relevant Jaccard similarity,” *Information Sciences*, vol. 483, pp. 53–64, 5 2019. [Online]. Available: <https://linkinghub.elsevier.com/retrieve/pii/S0020025519300325>
- [45] B. Zhu, Y. Jiang, M. Gu, and Y. Deng, “A GPU Acceleration Framework for Motif and Discord Based Pattern Mining,” *IEEE Transactions on Parallel and Distributed Systems*, vol. 32, no. 8, pp. 1987–2004, 8 2021. [Online]. Available: <https://ieeexplore.ieee.org/document/9343677/>
- [46] J. Zhu, Z. Wang, S. Wang, and S. Chen, “Moving Object Detection Based on Background Compensation and Deep Learning,” *Symmetry*, vol. 12, no. 12, p. 1965, 11 2020. [Online]. Available: <https://www.mdpi.com/2073-8994/12/12/1965>
- [47] M.-N. Chapel and T. Bouwmans, “Moving objects detection with a moving camera: A comprehensive review,” *Computer Science Review*, vol. 38, p. 100310, 11 2020. [Online]. Available: <https://linkinghub.elsevier.com/retrieve/pii/S157401372030410X>
- [48] H. Zhu, H. Wei, B. Li, X. Yuan, and N. Kehtarnavaz, “A Review of Video Object Detection: Datasets, Metrics and Methods,” *Applied Sciences*, vol. 10, no. 21, p. 7834, 11 2020. [Online]. Available: <https://www.mdpi.com/2076-3417/10/21/7834>
- [49] L. Jiao, F. Zhang, F. Liu, S. Yang, L. Li, Z. Feng, and R. Qu, “A Survey of Deep Learning-Based Object Detection,” *IEEE Access*, vol. 7, pp. 128 837–128 868, 2019. [Online]. Available: <https://ieeexplore.ieee.org/document/8825470/>
- [50] Z.-Q. Zhao, P. Zheng, S.-T. Xu, and X. Wu, “Object Detection With Deep Learning: A Review,” *IEEE Transactions on Neural Networks and Learning Systems*, vol. 30, no. 11, pp. 3212–3232, 11 2019. [Online]. Available: <https://ieeexplore.ieee.org/document/8627998/>
- [51] T. Jiang, J. L. Gradus, and A. J. Rosellini, “Supervised Machine Learning: A Brief Primer,” *Behavior Therapy*, 2020.
- [52] X. Wang, X. Lin, and X. Dang, “Supervised learning in spiking neural networks: A review of algorithms and evaluations,” *Neural Networks*, 2020.
- [53] Z. Zhou, R. Zhang, and D. Yin, “A strong feature representation for siamese network tracker,” *Multimedia Tools and Applications*, vol. 79, no. 35–36, pp. 25 873–25 887, 9 2020. [Online]. Available: <https://link.springer.com/10.1007/s11042-020-09164-2>
- [54] J. Peng, J. Li, and X. Shang, “A learning-based method for drug-target interaction prediction based on feature representation learning and deep neural network,” *BMC Bioinformatics*, vol. 21, no. S13, p. 394, 9 2020. [Online]. Available: <https://bmcbioinformatics.biomedcentral.com/articles/10.1186/s12859-020-03677-1>
- [55] Y. Xie, Z. Du, J. Li, M. Jing, E. Chen, and K. Lu, “Joint metric and feature representation learning for unsupervised domain adaptation,” *Knowledge-Based Systems*, vol. 192, p. 105222, 3 2020. [Online]. Available: <https://linkinghub.elsevier.com/retrieve/pii/S0950705119305489>
- [56] R. Garcia, R. Prados, J. Quintana, A. Tempelaar, N. Gracias, S. Rosen, H. Vågstøl, and K. Løvfall, “Automatic segmentation of fish using deep learning with application to fish size measurement,” *ICES Journal of Marine Science*, 2020.
- [57] C. C. Chang, Y. P. Wang, and S. C. Cheng, “Fish segmentation in sonar images by mask r-cnn on feature maps of conditional random fields,” *Sensors*, 2021.
- [58] N. F. F. Alshdaifat, A. Z. Talib, and M. A. Osman, “Improved deep learning framework for fish segmentation in underwater videos,” *Ecological Informatics*, vol. 59, p. 101121, 2020.
- [59] A. A. Jabri, A. Owens, and A. A. Efros, “Space-time correspondence as a contrastive random walk,” in *Advances in Neural Information Processing Systems*, 2020.
- [60] N. Araslanov, S. Schaub-Meyer, and S. Roth, “Dense Unsupervised Learning for Video Segmentation,” *IEEE*, 11 2021. [Online]. Available: <https://arxiv.org/abs/2111.06265v1>
- [61] N. Wang, W. Zhou, and H. Li, “Contrastive Transformation for Self-supervised Correspondence Learning,” *IEEE*, 12 2020. [Online]. Available: <https://arxiv.org/abs/2012.05057v1>
- [62] R. Liu, Z. Wu, S. X. Yu, and S. Lin, “The Emergence of Objectness: Learning Zero-Shot Segmentation from Videos,” *Advances in Neural Information Processing Systems*, vol. 16, pp. 13 137–13 152, 11 2021. [Online]. Available: <https://arxiv.org/abs/2111.06394v1>
- [63] A. Saleh, M. Sheaves, D. Jerry, and M. R. Azghadi, “Transformer-based Self-Supervised Fish Segmentation in Underwater Videos,” *IEEE*, 6 2022. [Online]. Available: <http://arxiv.org/abs/2206.05390>
- [64] N. A. Golilarz, H. Demirel, and H. Gao, “Adaptive Generalized Gaussian Distribution Oriented Thresholding Function for Image De-Noiseing,” *International Journal of Advanced Computer Science and Applications*, vol. 10, no. 2, 2019. [Online]. Available: <http://thesai.org/Publications/ViewPaper?Volume=10&Issue=2&Code=ijacsa&SerialNo=2>
- [65] Z. Teed and J. Deng, “RAFT: Recurrent All-Pairs Field Transforms for Optical Flow (Extended Abstract),” in *Proceedings of the Thirtieth International Joint Conference on Artificial Intelligence*. California: International Joint Conferences on Artificial Intelligence Organization, 8 2021, pp. 4839–4843. [Online].

- Available: <https://www.ijcai.org/proceedings/2021/662>
- [66] N. Xu, L. Yang, Y. Fan, J. Yang, D. Yue, Y. Liang, B. Price, S. Cohen, and T. Huang, "YouTube-VOS: Sequence-to-Sequence Video Object Segmentation," in *Lecture Notes in Computer Science (including subseries Lecture Notes in Artificial Intelligence and Lecture Notes in Bioinformatics)*, 2018.
- [67] Georgiou Giannis, "Mediterranean Fish Species," 2021. [Online]. Available: <https://www.kaggle.com/datasets/giannisgeorgiou/fish-species>
- [68] D. T. Nguyen, M. Dax, C. K. Mummadi, T. P. N. Ngo, T. H. P. Nguyen, Z. Lou, and T. Brox, "DeepUSPS: Deep robust unsupervised saliency prediction with self-supervision," in *Advances in Neural Information Processing Systems*, vol. 32, 2019.
- [69] L.-C. Chen, G. Papandreou, I. Kokkinos, K. Murphy, and A. L. Yuille, "Deeplab: Semantic image segmentation with deep convolutional nets, atrous convolution, and fully connected crfs," *PAMI*, vol. 40, no. 4, pp. 834–848, 2018.
- [70] P. Krähenbühl and V. Koltun, "Efficient inference in fully connected crfs with gaussian edge potentials," in *Advances in neural information processing systems*, 2011, pp. 109–117.
- [71] X. Wang, R. Zhang, T. Kong, L. Li, and C. Shen, "SOLOv2: Dynamic and fast instance segmentation," in *Advances in Neural Information Processing Systems*, vol. 2020-December, 2020.
- [72] X. Wang, T. Kong, C. Shen, Y. Jiang, and L. Li, "SOLO: Segmenting Objects by Locations," in *Lecture Notes in Computer Science (including subseries Lecture Notes in Artificial Intelligence and Lecture Notes in Bioinformatics)*, 2020, vol. 12363 LNCS, pp. 649–665. [Online]. Available: https://link.springer.com/10.1007/978-3-030-58523-5_38
- [73] E. Shelhamer, J. Long, and T. Darrell, "Fully Convolutional Networks for Semantic Segmentation," *IEEE Transactions on Pattern Analysis and Machine Intelligence*, vol. 39, no. 4, pp. 640–651, 4 2017.
- [74] A. Neubeck and L. Van Gool, "Efficient Non-Maximum Suppression," in *18th International Conference on Pattern Recognition (ICPR'06)*, vol. 3. IEEE, 2006, pp. 850–855. [Online]. Available: <http://ieeexplore.ieee.org/document/1699659/>
- [75] OpenCv, "OpenCV Library," *OpenCV Website*, p. All, 2014. [Online]. Available: <https://opencv.org/about.html>
- [76] A. Bewley, Z. Ge, L. Ott, F. Ramos, and B. Upcroft, "Simple Online and Realtime Tracking," *Proceedings - International Conference on Image Processing, ICIP*, vol. 2016-August, pp. 3464–3468, 2 2016. [Online]. Available: <http://arxiv.org/abs/1602.00763><http://dx.doi.org/10.1109/ICIP.2016.7533003>
- [77] R. E. Kalman, "A New Approach to Linear Filtering and Prediction Problems," *Journal of Basic Engineering*, vol. 82, no. 1, pp. 35–45, 3 1960. [Online]. Available: <https://asmedigitalcollection.asme.org/fluidsengineering/article/82/1/35/397706/A-New-Approach-to-Linear-Filtering-and-Prediction>
- [78] H. W. Kuhn, "The Hungarian method for the assignment problem," *Naval Research Logistics Quarterly*, vol. 2, no. 1-2, 1955.
- [79] Tie Liu, Zejian Yuan, Jian Sun, Jingdong Wang, Nanning Zheng, Xiaoou Tang, and Heung-Yeung Shum, "Learning to Detect a Salient Object," *IEEE Transactions on Pattern Analysis and Machine Intelligence*, vol. 33, no. 2, pp. 353–367, 2 2011. [Online]. Available: <http://ieeexplore.ieee.org/document/5432215/>
- [80] A. Paszke, S. Gross, F. Massa, A. Lerer, J. Bradbury, G. Chanan, T. Killeen, Z. Lin, N. Gimelshein, L. Antiga, A. Desmaison, A. Köpf, E. Yang, Z. DeVito, M. Raison, A. Tejani, S. Chilamkurthy, B. Steiner, L. Fang, J. Bai, and S. Chintala, "PyTorch: An imperative style, high-performance deep learning library," in *Advances in Neural Information Processing Systems*, 2019.
- [81] D. P. Kingma and J. Ba, "Adam: A method for stochastic optimization," *arXiv preprint arXiv:1412.6980*, 2014.
- [82] X. Chen, R. Girshick, K. He, and P. Dollár, "TensorMask: A Foundation for Dense Object Segmentation," in *2019 IEEE/CVF International Conference on Computer Vision (ICCV)*, vol. 2019-October. IEEE, 10 2019, pp. 2061–2069. [Online]. Available: <https://ieeexplore.ieee.org/document/9010024/>
- [83] T. Y. Lin, M. Maire, S. Belongie, J. Hays, P. Perona, D. Ramanan, P. Dollár, and C. L. Zitnick, "Microsoft COCO: Common objects in context," in *Lecture Notes in Computer Science (including subseries Lecture Notes in Artificial Intelligence and Lecture Notes in Bioinformatics)*, 2014.